# INSTRUMENTED FLIP TEST AND STATIC PRESSURE INFLUENCE ON THE ONSET VELOCITY AND FREQUENCY ON AN INDUSTRIAL SCALE

Matthieu Decuupere, David Charliac, Jen-Philippe Roques, Alexandre Karnikian, Gaëtan Galeron, Pierre-Olivier Mattei, M. Amielh

**Proceedings of the ASME 2018 37th International Conference on Ocean, Offshore and Arctic Engineering**
**OMAE2018**
**June 17-22, 2018, MADRID, SPAIN**

**2018-77905**

# INSTRUMENTED FLIP TEST AND STATIC PRESSURE INFLUENCE ON THE ONSET VELOCITY AND FREQUENCY ON AN INDUSTRIAL SCALE

**M. DECUUPERE**
TechnipFMC - France
matthieu.decuupere@technipfmc.com

**D. CHARLIAC**
TechnipFMC - France
david.charliac@technipfmc.com

**JP. ROQUES**
TOTAL E&P - France
jean-philippe.roques@total.com

**A. KARNIKIAN**
TOTAL E&P - France
alexandre.karnikian@total.com

**G. GALERON**
TOTAL E&P - France
gaetan.galeron@centrale-marseille.fr

**PO. MATTEI**
LMA, CNRS,
Aix Marseille Univ,
Centrale Marseille - France
mattei@lma.cnrs-mrs.fr

**M. AMIELH**
IRPHE, CNRS,
Aix Marseille Univ,
Centrale Marseille - France
amielh@irphe.univ-mrs.fr

## ABSTRACT

Since the early 2000, Flow Induced Pulsations (FLIP) has been more and more encountered on platforms. This phenomenon generates high acoustic pressure pulsations that may cause noises up to one hundred and ten dB and significant fatigue stress levels in small piping either at topside or subsea equipment. The source of the phenomenon is inside of the flexible pipe but FLIP has no effect on it. Nevertheless, in case of FLIP experience companies may have to reduce their flow rate. Therefore, FLIP must be understood in order for the companies to avoid this constraint.

In this frame, a FLIP test was performed with protagonists who are involved in the understanding of this phenomenon. The test was done in 2016 at CESAME Poitiers (France) in an eighteen meter-long and six-inch flexible pipe on an air open loop. The prototype was fully instrumented and pressures up to forty bars were tested and mass flow rates up to 6 $kg.s^{-1}$ to reproduce the FLIP phenomenon.

The test setup and signals analysis are presented in this paper. Moreover, FLIP onset velocities and frequencies are compared with TechnipFMC models. As a conclusion of this paper pressure influence for the six-inch tested on the FLIP initiation will be presented.

## INTRODUCTION

A FLIP test was conducted end of 2016 at CESAME Poitiers in collaboration between three main stakeholders: TOTAL / TechnipFMC / CNRS (LMA+IRPHE). This collaboration aimed at reproducing FLIP phenomenon with a complete flexible pipe equipped with actual end-fittings that would be the most representative of an actual riser configuration. The test campaign also aimed at getting a better understanding about the nature of the acoustic wave itself generated inside a flexible pipe that is subjected to FLIP phenomenon. That is why a certain number of accurate and sophisticated sensors was used to monitor at best the phenomenon. Figure 1 shows the corrugated inside of the tested flexible pipe.

*Figure 1 – View of the inside of the tested rough bore flexible pipe*

This article will focus on the presentation of the FLIP test campaign, the test setup and more specifically on the test results.

## NOMENCLATURE

| | |
|---|---|
| dB | DeciBels |
| FLIP | FLow Induced Pulsations |
| ID | Internal Diameter [m] |
| L | Total pipe length [m] |
| P | Static pressure [Pa] |
| PSD | Power Spectral Density |
| $Q_m$ | Mass flow rate [kg.s$^{-1}$] |
| R | Inner flexible pipe radius [m] |
| U | Average flow velocity [m.s$^{-1}$] |
| $\Delta P_{losses}$ | Other pressure losses [Pa] |
| $\Delta P_{measured}$ | Pressure drop measured during test [Pa] |
| $\Delta P_{viscous}$ | Viscous pressure loss [Pa] |
| $\lambda_{RB}$ | Darcy friction factor for rough bore flexible viscous losses [-] |
| $\rho$ | Density [kg.m$^{-3}$] |

## PHENOMENON DESCRIPTION

Today gas fields are more and more important. A flexible pipe may be seen as a succession of cavities, it may then be the root cause of an acoustic phenomenon: FLIP (for Flow Induced Pulsations) [Ref. 1, 2, 3]. At each cavity, a shear layer is generated in which vortices are shed from the leading edge to the downstream edge. When these vortices impinge the downstream edge of the corrugation they may be source of sound depending of their strength and if there is any frequency lock-in. The onset of the phenomenon is highly dependent on pressure, temperature for a given fluid and flexible pipe geometry.

## TESTS

### Test description:

This test campaign was conducted in 2016 at CESAME Poitiers and aimed at studying more in details FLIP phenomenon. Each phase of the test campaign was witnessed by a third-party. One goal of the test was to reproduce FLIP phenomenon with an actual complete flexible pipe on an industrial scale. In order to complete all phases both flow directions had to be tested for a complete range of pressure and mass flow rates. Tested geometry was an eighteen-meter-long rough bore flexible pipe (i.e. including an actual interlocked carcass) with an internal diameter of six inches. The prototype from industrial manufacturing had real end-fittings making it very similar to an actual riser configuration. Figure 2 shows a general overview of the test facility and flexible pipe.

*Figure 2 – Overview of the test facility and flexible pipe*

### Test monitoring:

At each of its end, the riser was equipped with couplers (Fig. 3a) on each of which were fixed one hot-film velocity sensor (HW1 and HW2, Dantec Dynamics), a temperature probe, a pressure sensor (Kulite) and three GRAS probe microphones separated by 0.4 m and 0.5 m (Fig. 3b). Connections to sensor probes are collected in a control station (Fig. 3c). All the signal were digitalized using a synchronous multi-channels analyser NetDB (01dB-Metravib) at a sampling rate of 25 600 Hz. For each test, the velocity of the flow inside the pipe was increased step by step until the desired maximum and then maintained constant to allow long time records. The duration of each test approaches ten minutes.

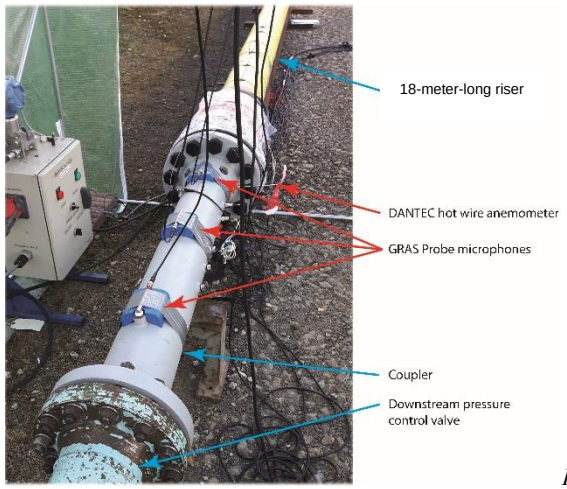


*Fig. 3a)*

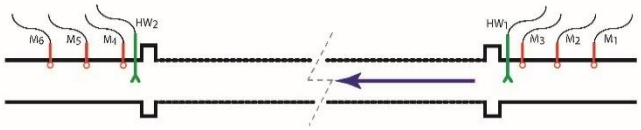


*Fig. 3b)*

*Fig.3 c)*

*Figure 3 – Data acquisition set-up: a) The downstream equipped coupler, b) The 6 microphones and the two hot wire anemometers c) The control station gathering probes signals.*

**Test setup :**

The test was performed with fully dry gas: dry air. The eighteen-meter-long corrugated flexible is supplied with pressurized air at 200 bar from a 200 $m^3$ reservoir. A smooth piping of approximately 40 meters connects the riser to the pressure tank. A downstream pressure valve control the inside flexible pressure during tests. The series of tests was conducted for internal pressures varying from 1 bar to approximately 40 bars and flow velocity varying from 5 $m.s^{-1}$ to 80 $m.s^{-1}$. Figure 4 highlights an overview of the test setup.

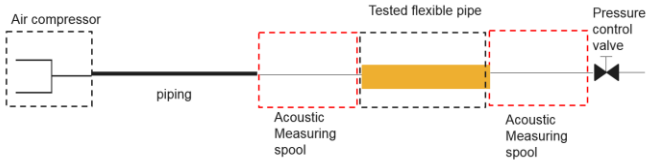


*Figure 4 – Overview of the test setup*

To experience FLIP phenomenon mass flow rate $Q_m$ had to be fixed (imposed by CESAME). Pressure had to be swept to travel the whole matrix defined in Table 1 . To get an increasing flow velocity at a given mass flow rate pressure had to be driven in a decreasing sweep way. Decreasing pressure implies a density decrease and thus a velocity increase at a given mass flow rate.

Table 1 shows the global limits of the test campaign in terms of mass flow rate, static average pressure and density. Upper limits were set by the test facilities capacities. Global test matrix included more than thirty triplets (P, T, $Q_m$).

| | $Q_m$ [$kg.s^{-1}$] | P [bar] | ρ [$kg.m^{-3}$] |
|---|---|---|---|
| Mini | 0 | 1 | 1.2 |
| Maxi | 8.3 | 40 | 46 |

*Table 1 – Test matrix*

**Test results:**

## 1. Post-process of pressure and velocity signals

As the database is very large, a specific configuration when FLIP arose is here chosen to illustrate the emergence of the phenomenon. In the following analysis, the maximum flow velocity inside the pipe was close to 70 $m.s^{-1}$ and the internal pressure was close to 1.5 bar.

### *a. Turbulence and acoustics: velocity measurements by hot-wires*

Both hot-films are positioned on the axis of couplers, just upstream and downstream of the flexible. The dimensions of the sensitive part of each hot-film (55R01 type) are 70 µm in diameter with a 0.5 µm thickness quartz coating and 1.25 mm in length. The overheat was adjusted to $a_w = 0.6$. The calibration of hot-films is established for each test with in-situ reference velocities given by generating conditions provided by CESAME. Thanks to a high-pressure seal system (Swagelock), the hot-films were operational for the whole pressure range up to 40 bar.

For the present experimental conditions, the turbulence level at the downstream end of the riser is in the range 2-3.5%, in a good agreement with axial turbulence in fully turbulent developed pipe flows. An increasing of 40% of turbulence intensity is registered between the upstream and downstream ends of the flexible. As it was checked in previous laboratory measurements [Ref. 4], hot wire is not only sensitive to turbulence but also to acoustics. Figure 5 presents the evolution of the power spectral density (PSD) estimated from velocity hot-wire signals when the reference velocity increases from 50 to 70 $m.s^{-1}$. These results show that many frequencies are caught by upstream hot-wire, probably due to the supplying system including air compressor and some bends on the upstream piping. These large peaks do not appear on the PSD of downstream hot-wire, indicating that the flexible behave like a filter for upstream flow turbulence. When the velocity reaches around 60 $m.s^{-1}$ sharp peaks of frequencies emerge and, this, clearly on the downstream velocity PSD. These singular frequencies (1250, 2150, 2600 Hz) are associated to the FLIP phenomenon and are confirmed by the following acoustic pressure analyses.

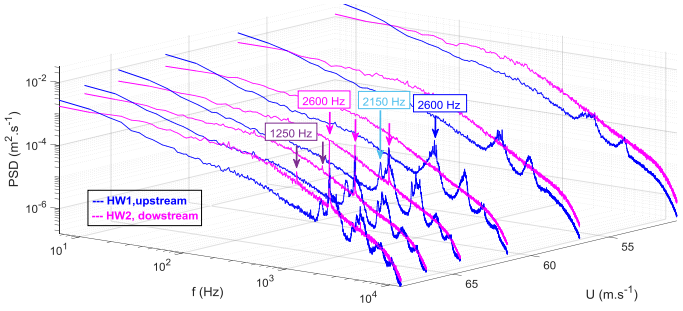


*Figure 5 – Power spectral density of velocity signals from upstream and downstream hot-wires for an 80° aperture of control valve (test 13, 1.1bar<$P_{upstream}$<1.6 bar )*

### *b. Analysis of acoustic pressure signals*

The first analysis of the recorded signals reveals that during the whistling process, not only a strong acoustics field (170 dB SPL) inside the riser appears at frequencies that are close to the transverse acoustic resonance of the pipe (i.e. 1250 Hz, 2110 Hz and 2650 Hz), but also that this sound field shows significant time and frequency fluctuations. Then, it was decided to analyze these signals using Gabor-wave let time-frequency and Hilbert transform analysis to catch the fine structure of the whistling.

#### *Time frequency analysis*

A Gabor wavelet time-frequency analysis is given in Figure 6. It corresponds to 10 seconds of the signal recorded on microphone 4 (the downstream riser's end closest microphone) during the maximum whistling of the riser.

The signal is clearly composed by two main frequency components around the first modes of the riser (i.e. 1250 Hz and 2500 Hz for a riser with constant radius R=7.62 cm). It is also obvious that this whistling processes significant variations in time and frequency.

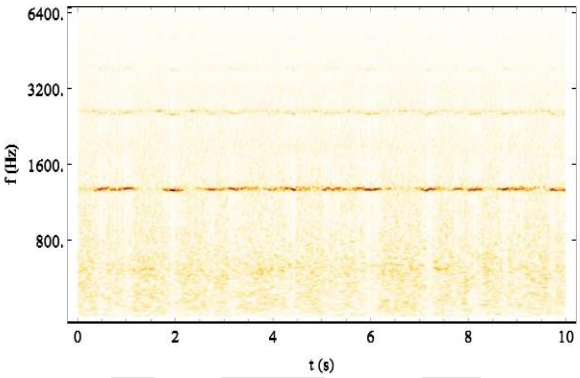


*Figure 6 – Wavelet analysis during the whistling phase recorded on microphone N°4.*

To see it more clearly, one applies a Hilbert transform of the signal filtered around the first mode to compute its instantaneous frequency [Ref. 6]. The result is given in Figure 7. In that case, the amplitude is normalised to the maximum recorded during that interval and the curve is plotted with an intensity of the grey corresponding to its amplitude. This helps to see that both amplitude and frequency vary strongly, even on that short time interval.

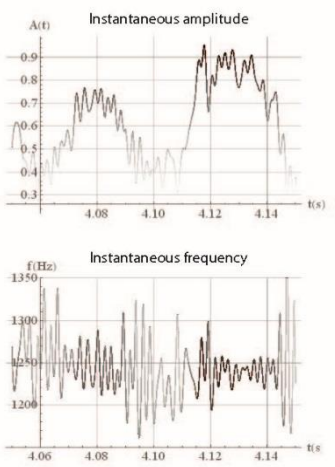


*Figure 7 – Instantaneous amplitude and frequency during the whistling phase recorded on microphone N°4.*

As it is easy to see in Figure 7, the frequency fluctuates around that of the first transversal mode ($f \in [1190; 1290]$ Hz) with a fluctuation corresponding quite exactly to the variation of the inner radius caused by the corrugation ($R \in [7.4; 8.1]$ cm).

#### *Correlations analysis*

In the following, a Pearson's correlation analysis is conducted between two microphones of the downstream coupler. To save place, only results for the correlation study between the microphones 4 and 5 are provided. To do this, for the whole test duration, one computes the correlation between the signal recorded by the microphone 5 and that recorded by microphone 4 shifted by n samples, with $n \in [1, 25600]$, corresponding to an estimation of correlation of a maximal time shift of 1 second. Because of the whistling, the correlation oscillates at a period corresponding to the frequency of the whistling as shown in Figure 8. This figure presents the correlation between microphones 4 and 5, calculated between the times 400 and 450 seconds, corresponding to the maximum of the riser whistling. It is observed that the time of the first correlation maximum gives a length ($l = v. T$) based on the speed of the flow of almost 2 cm (exactly 1.7) and that the time of the maximum correlation gives a length based on the flow velocity of about 0.5 meter (inter-microphone spacing is 0.4m).

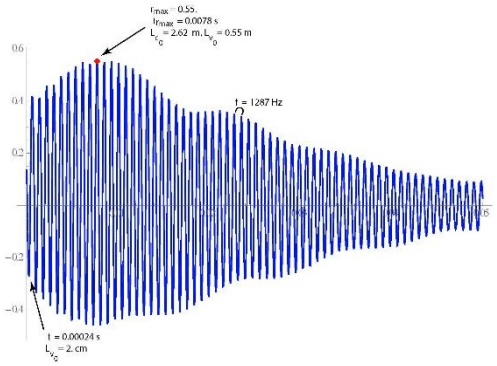


*Figure 8 –Pearson's correlation.*

This indicates that the signal measured at the microphones propagates at the speed of the flow and not at the wave velocity for this particular correlation calculation. To verify that this remains true for the whole signal, this operation had been repeated for all the whistling moments, separating them by 1 second. For the two maxima of interest, the first one is given in Figure 8 and the absolute one is given in Figure 9.

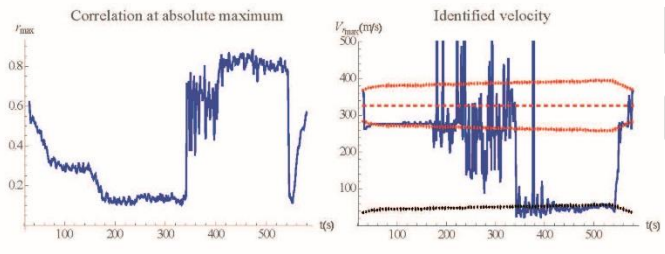


*Figure 9. – First correlation maximum. Lc =0.022 m.*

The time corresponding to these two extrema is used to deduce a characteristic speed (obtained by dividing a characteristics $d_c$ distance by this time). Two distances were tested: the pitch of the corrugation $L_c$ =0.022 m in Figure 9 and the inter-microphone distance: $L_c$ =0.4 m in Figure 10. The whistling starts around t = 340 s and ends close to t = 550 s. In these two figures, the dotted red curve corresponds to the wave velocity and the other two red curves to the wave velocity corrected by plus or minus the convective flow velocity, plotted in black dotted curve.

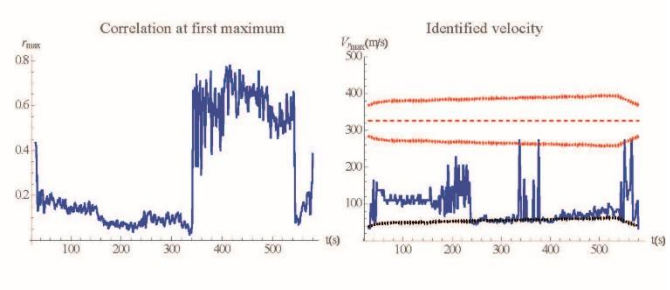


*Figure 10 –Absolute correlation maximum. Lc =0.4 m.*

In these two figures, it is obvious that the correlation is significant only during whistling. Figure 9 reveals that the first correlation maximum depends only on the corrugation size, confirming that the whistling is strongly dependent of the corrugations. Figure 10 confirms that during whistling the signal propagates along the pipe at the convective flow velocity while its frequency corresponds to a transverse acoustics resonance, which indicates a transverse propagation at wave speed, five times greater than that of convective flow.

## 2. Comparison between test results and model approached in [Ref. 5].

The model approached in [Ref. 5] was used to predict and compare test results. The graph here-below in Figure 11 shows the tested average flow velocities versus calculated onset velocities. For each calculated green point no onset was observed in Fast Fourier Transform post-processed graphs. For each calculated red point, FLIP was clearly observed in FFT post-processed graphs such as shown in Figure 12. For each orange point FLIP observation is questionable (small appearances were noticed but nothing major).

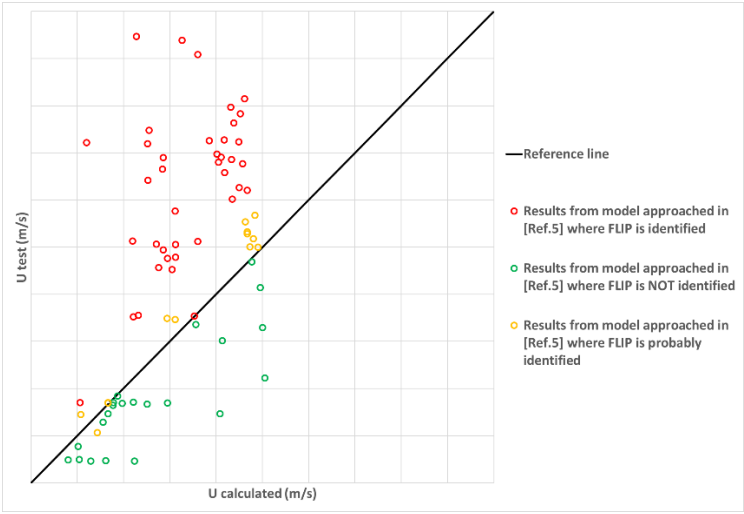


*Figure 11 – Comparison between post-processed test results and model approached in [Ref. 5]*

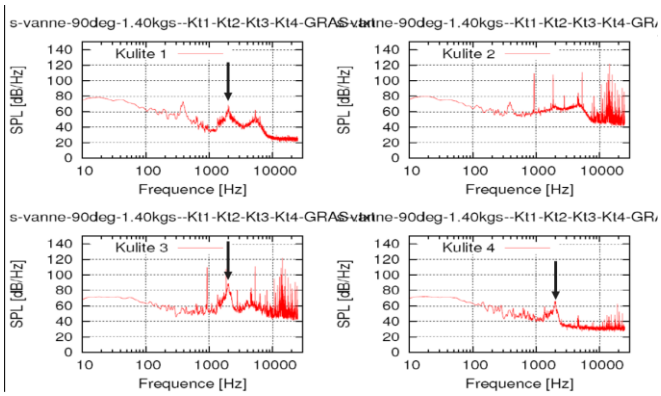


*Figure 12 – FFT post-processed instantaneous pressure*

More than thirty triplet of (P, T, $Q_m$) were tested and model approached in [Ref. 5] is found consistent after post-processing in terms of onset velocities and frequencies.

## 3. Onset criterion based on pressure drop measurement

In this section three different kind of pressure loss will be approached:

- "Viscous pressure loss": pressure loss due to internal viscous friction losses. Viscous losses may be calculated thanks to Darcy-Weisbach equation: $\Delta P_{viscous} = \frac{1}{2} \cdot \lambda_{RB} \cdot \rho \cdot U^2 \cdot \frac{L}{ID}$. And $\lambda_{RB}$ is calculated thanks to an in-house model.
- "Other pressure loss" $\Delta P_{losses}$: pressure loss due to all other energy losses such as acoustic, thermal and radiation. But, thermal and radiated losses are neglectable in front of acoustic ones for the tested conditions.
- "Total pressure loss" $\Delta P_{measured}$ which is the total effective pressure drop measured during test.

Therefore, one may write:

$$\Delta P_{measured} = \Delta P_{viscous} + \Delta P_{losses}.$$

Thus,

$$\Delta P_{losses} = \Delta P_{measured} - \frac{1}{2} \cdot \lambda_{RB} \cdot \rho \cdot U^2 \cdot \frac{L}{ID}.$$

$\Delta P_{measured}$ was accurately measured thanks to pressure sensors installed on the upstream and downstream measuring spools. Moreover, when $\lambda_{RB}$ is accurately preliminary assessed a clear indicator of onset may be derived (i.e. onset occurs if $\Delta P_{measured} > \Delta P_{viscous}$). Applying this concept at 1 bar-ish it may be found out that experimental onset would be between 55 and 62 m.s$^{-1}$ as presented in Figure 13. This result is in line with results provided by hot wire probes shown in Figure 5 of the present paper. Moreover, FLIP model approached in [Ref. 5] would provide an onset velocity at approximately 56 m.s$^{-1}$. All these elements are consistent.

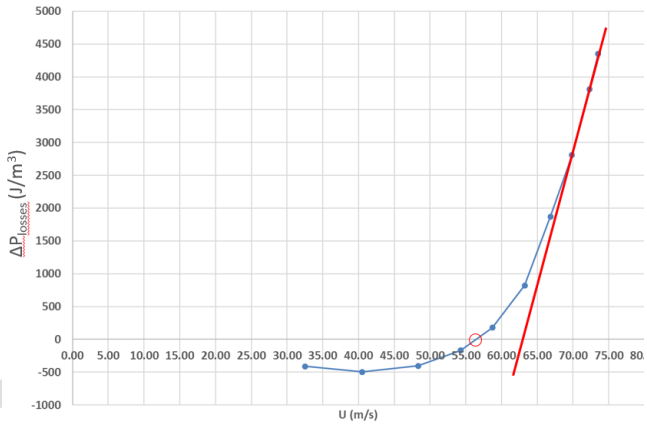


*Figure 13 – $\Delta P_{losses}$ versus U at 1 bara*

Thanks to this post-processing onset criterion, it was confirmed that the onset velocity decreases when pressure (i.e. density) increases such as shown in Figure 14.

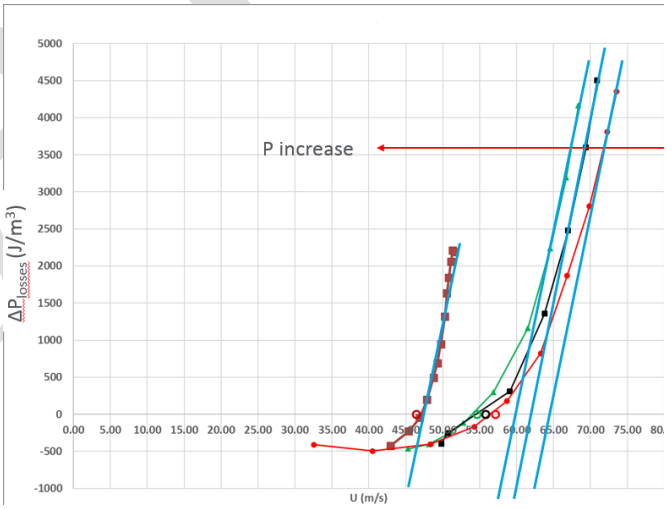


*Figure 14 - $\Delta P_{losses}$ versus U from 1 bara to 2 bara*

## CONCLUSION

In conclusion, a significant test campaign was carried out with an actual complete flexible pipe on an industrial scale. FLIP phenomenon was successfully reproduced with dry air.

Thanks to an adequate monitoring FLIP phenomenon was easily captured. This allowed a better understanding of the nature of the very high level fluctuating pressure field inside of the rough bore flexible pipe. It was noticed that rough bore flexible pipe mainly whistles with its transverse acoustic modes while the fluctuating pressure signal propagates at convective flow velocity.

Moreover, FLIP model presented in Ref. [5] enabled an accurate screening of the pressures and mass flow rates to be targeted and an acceptable prediction of onset velocities and frequencies.

Analysis based on pressure loss examination was also found efficient to detect FLIP onset, as illustrated in Figures 13 and 14.

Such a successful test campaign was possible thanks to a strong partnership and collaboration between TechnipFMC, TOTAL and CNRS (LMA and IRPHE).

## ACKNOWLEDGEMENTS

The authors acknowledge TechnipFMC, TOTAL and CNRS (LMA and IRPHE) for allowing them to prepare this paper, CESAME for their test facilities disposal and Bureau Veritas Paris for their test witnesses.

## REFERENCES

[Ref. 1] W. Burstyn, Z. Tech. Phys. Leipzig. 3 (1922), pp. 179–180, Eine neue Pfeife (a new pipe).

[Ref. 2] P. Cermak, Phys. Z. 23 (1922), pp. 394–397, Über die Tonbildung bei Metallschläuchen mit eingedrücktem Spiralgang [On the sound generation in flexible metal hoses with spiraling grooves].

[Ref. 3] B. Rajavel and M.G. Prasad, Appl. Mech. Rev. 65 (2013), pp. 050000/1–050000/24, Acoustics of corrugated pipes: A review.

[Ref. 4] M. Amielh, F. Anselmet, Y. Jiang, U. Kristiansen, P.O. Mattei, D. Mazzoni, C. Pinhède, Journal of Turbulence, 15:10, 650-676, 2014, Aeroacoustic source analysis in a corrugated flow pipe using low-frequency mitigation.

[Ref. 5] M. Décuupère, D. Charliac, S. Legeay. OMAE 2017-61324, Flow Induced Pulsations (FLIP) in rough bore gas flexible pipes, tests and model.

[Ref. 6] B. Boashash, Parts 1 and 2, Proc. IEEE 80(4) (1992), pp. 520-568, Estimating and interpreting the instantaneous frequency of a signal.